Liquid Crystals
Publication details, including instructions for authors and subscription information:
http://www.informaworld.com/smpp/title~content=t713926090

Collective dynamic modes in ferroelectric liquid crystal-aerosil dispersions

Stanisław A. Różański[a]; Jan Thoen[a]
[a] Laboratorium voor Akoestiek en Thermische Fysica, Departement Natuurkunde en Sterrenkunde, Katholieke Universiteit Leuven, B-3001 Leuven, Belgium

To cite this Article Różański, Stanisław A. and Thoen, Jan(2005) 'Collective dynamic modes in ferroelectric liquid crystal-aerosil dispersions', Liquid Crystals, 32: 3, 331 — 340
To link to this Article: DOI: 10.1080/02678290500033760
URL: http://dx.doi.org/10.1080/02678290500033760

Liquid Crystals, Vol. 32, No. 3, March 2005, 331–341

Taylor & Francis
Taylor & Francis Group

Collective dynamic modes in ferroelectric liquid crystal-aerosil dispersions

STANISŁAW A. RÓŻAŃSKI and JAN THOEN*

Laboratorium voor Akoestiek en Thermische Fysica, Departement Natuurkunde en Sterrenkunde, Katholieke Universiteit Leuven, Celestijnenlaan 200D, B-3001 Leuven, Belgium

(*Received 28 June 2004; accepted 28 September 2004*)

The influence of the concentration of hydrophilic aerosil particles on the collective dynamic modes of the ferroelectric liquid crystal *S*-(-)-2-methylbutyl 4-*n*-nonanoyloxybiphenyl-4′-carboxylate near the SmA–SmC* phase transition is investigated by means of dielectric spectroscopy in the frequency range 10^{-2}–10^{7} Hz. For aerosil densities ρ_s=0.025, 0.05, 0.08 and 0.15 g cm^{-3} considerable changes in the dielectric intensities of Goldstone and soft modes are observed. The characteristic frequency of the Goldstone mode slightly increases with increasing concentration of aerosil. The frequency degeneracy occurring in the SmA–SmC* phase transition is lifted in the presence of aerosil and an increase in the frequency gap is observed. Complete disappearance of the Goldstone mode at ρ_s=0.20 g cm^{-3} occurs, along with significant broadening of the soft mode. The results are interpreted as an effect of structure, surface interactions and length scale of the helix in disordered confinement.

1. Introduction

Soft matter and in particular liquid crystals (LCs) are characterized by a strong response to relatively weak perturbations. As in liquid phases, liquid crystals constitute systems which are very well suited for investigation of general aspects of confinement effects and random field effects on systems having different types of long range order (positional and/or orientational). The confinement of LCs in various porous matrices, or filling them with inclusions, have been extensively investigated [1]. Moreover, LCs exhibit many phase transitions, which provides excellent opportunities to study confinement and random field effects on the delicate balances at these transitions. The study of physical properties of ferroelectric liquid crystals (FLCs) confined to different porous matrices or filled with inclusions is also an area of growing interest [2–13]. The fast switching and promising application of FLC displays attracts attention to an understanding of the physical mechanisms of surface-induced ordering and geometrical confinement of a FLC. The thermodynamic properties of a FLC, especially near the second order SmA–SmC* phase transition, can be significantly modified and affected by geometrical restrictions. Besides the molecular processes observed in a FLC, two additional collective relaxation processes related to fluctuations of the azimuthal angle ϕ (Goldstone mode) and tilt angle θ (soft mode) are present. The double-degenerate soft mode in the smectic A phase splits in the phase transition into a soft amplitude mode and a Goldstone mode which is related to the formation of a helical superstructure in the SmC* phase. The helix in the ferroelectric SmC* phase is strongly influenced and deformed by surface interactions, causing a substantial change in the dynamics of the Goldstone mode.

For the investigation and probing of the surface interactions of LCs in various confinements, several experimental methods have been performed, such as calorimetry [14–20], deuteron NMR [21–25], dielectric spectroscopy [1–9, 26–36], X-ray scattering [2, 15, 37–39], atomic force microscopy (AFM) [40, 41] and dynamic light scattering [42, 43]. In particular, broadband dielectric spectroscopy (BDS) is a very convenient and proven method for the investigation of complex systems. It covers an extremely broad range of frequencies, from 10^{-6} Hz to about 10^{11} Hz and temperatures from 100 to 800 K. Hence, this method is very suitable for the study of molecular and collective relaxation processes in a LC. The changes of dielectric strengths, relaxation times and shape of relaxation processes provide valuable information on interactions with the structure of the porous matrices or inclusions.

Liquid crystals can be adsorbed in porous matrices with varying degree of randomness, such as Anopore

*Corresponding author. Email: jan.thoen@fys.kuleuven.ac.be

Liquid Crystals
ISSN 0267-8292 print/ISSN 1366-5855 online
http://www.tandf.co.uk/journals
DOI: 10.1080/02678290500033760

and Nuclepore membranes with well separated cylindrical pores [44], Synpor and Millipore filters with a complex inner structure of interconnected voids [32, 45, 46], porous glasses (Vycor, CPG) with narrow pore size distribution but random orientation of cavities [47–49], and silica aerogels with irregularly shaped cavities and broad size distribution [19]. Moreover, dispersions or gels can be obtained in LCs filled with solid particles, hydrogen bonding additives, or polymerized photoreactive monomers. The ferroelectric mesogens can be encapsulated in a polymer (PDLC), stabilized by a network in the sample or by creating a physical gel [50]. In particular, the effect of silica aerosil particles on different liquid crystal phases has received a great amount of theoretical [51–54] and experimental attention [14–17, 26–29]. Silica particles covered with hydroxyl groups can hydrogen bond in a network, allowing the introduction of controlled disorder in LCs.

Several dielectric studies of the homologous series of *n*-cyanobiphenyl liquid crystals (*n*CB, with $n=5$–8) confined in porous adsorber materials [30–34], as well as dispersed with silica aerosil particles [26–29], have been performed to reveal effects of surface interaction, shape and finite size on the molecular dynamics of relaxation processes in different mesophases. Moreover, other mesogens were used in dielectric experiments to probe the influence of silica inclusions [35]. The relaxation processes present in bulk 5CB and 8CB are also observed in porous matrices with relaxation times almost uninfluenced by confinement, except in the region of the isotropic–nematic phase transition. In microporous glasses additional processes were identified, with Maxwell–Wagner polarization and retarded dynamics of molecules at the pore walls. A significant deviation from Arrhenius characteristics of the temperature dependence of the relaxation time was observed [34]. Depending on the silica density ρ_s (weight of silica per cm^3 of LC) numerous changes in dielectric spectra of 6CB, 7CB and 8CB were found: (i) relaxation processes in the mixture are of non-Debye type and for high concentration ($\rho_s > 0.825\,g\,cm^{-3}$) follow the Fogel–Fulcher–Tamman law; (ii) in the low frequency range, a new relaxation process is observed due to the hindered rotation of molecules located in the surface layer. It should be noted that with increasing concentration of aerosil particles three qualitatively different regimes can be distinguished [2, 15]: (i) diluted regime ($\rho_s \sim 0.01\,g\,cm^{-3}$) with almost isolated aggregates of aerosil in the LC; (ii) soft regime ($0.01\,g\,cm^{-3} < \rho_s \sim 0.1\,g\,cm^{-3}$), where a hydrogen-bonded, very responsive gel-like structure is formed; (iii) stiff regime for larger concentrations of aerosil similar to the rigid aerogel structure.

It has been shown in previous experiments that confinement can considerably influence the collective dynamic processes of FLCs [4, 5, 36]. The helical pitch gives some inherent scale for estimation of the efficiency of boundary conditions on the orientational arrangement and collective dynamic processes. In the cylindrical geometry of Anopore membranes embedded with FLCs (DOBAMBC, CE8) possessing small spontaneous polarization $\mathbf{P}_s$ but a quite large helical pitch (on the pore size scale), neither the Goldstone nor the soft modes were detected dielectrically [5, 36]. In the fractal-like structure of Synpor nitrocellulose membranes filled with DOBAMBC [4] and 4-octyloxy-4-(2-methylbutyloxy)carbonylphenyl benzoate [5], no Goldstone mode was observed in either material, although the soft mode was present in the second case. Moreover, in the short pitch and large $\mathbf{P}_s$ material C7 confined to mesoporous membranes, the soft and Goldstone modes were evidently present [4, 55]. Nevertheless, in the Synpor matrix, the Goldstone mode had reduced strength, broadened with respect to the bulk and shifted by more than one decade. In the cylindrical geometry of untreated Anopore filters, a collective process in the MHz region was detected instead of a phason bulk relaxation [55]. The nature of this process originates from a relaxation of flexoelectric polarization near the splayed regions at the pore walls. In other dielectric measurements it was shown that in membranes treated with palmitic acid the relaxation frequency of both the soft and Goldstone modes increases, the latter as much as by 4×10^2 times [2]. An additional relaxation process arising from the interfacial layer was also reported in a highly porous aerogel structure containing FLC [7]. The effect of dispersed silica aerosil on the SmA–SmC* phase transition was already investigated in the ferroelectric liquid crystal CE8. It was found that for $\rho_S < 0.176\,g\,cm^{-3}$ the Goldstone characteristic frequency f_G exhibits bulk-like behaviour. However, for $\rho_S = 0.176\,g\,cm^{-3}$ the Goldstone mode completely disappears and the soft mode anomalously broadens. In some cases a small increase in the Goldstone mode frequency for $\rho_S < 0.111\,g\,cm^{-3}$ has been observed [3]. This mesogen was also previously used in dielectric experiments with mesoporous membranes [36, 56], where a significant influence on the collective dynamic processes was observed.

These previous measurements were restricted only to matrices with a limited range of diameters of the pore, which prevented a more detailed investigation of the physical mechanisms leading to a reduced dynamic behaviour of the FLC in confinement. However, in aerosil–FLC dispersions, random disorder seems to

be introduced and controlled more easily, which can lead to a more adequate and complete explanation of the observed modifications of collective relaxation processes.

In a bulk FLC several anomalies are observed in a narrow temperature range below the SmA–SmC* phase transition temperature T_{AC}, such as a distinct asymmetric maximum of the helical pitch [12, 57], the reentrant behaviour of critical electric and magnetic fields [58, 59], and a maximum in dielectric susceptibility or lift of the double degeneracy of the soft mode [60]. Particularly interesting is the question as to what happens with the dynamics of collective processes in the SmA–SmC* phase transition when introducing random disorder in a controlled way to the liquid crystal.

In this study, the dynamics of collective processes of a ferroelectric liquid crystal dispersed with different concentrations of aerosil particles near the SmA–SmC* phase transition is investigated by dielectric spectroscopy. The influence of aerosil inclusions on the collective relaxation processes is discussed taking into account the hydrogen-bonded structures formed in the LC, the influence of interactions with hydrophilic surfaces, and the finite size effects on the formation of helical superstructure in the ferroelectric phase.

2. Experimental

Broadband dielectric spectroscopy has been employed to study the influence of aerosil particle concentrations on the collective dynamic modes of a FLC near the SmA–SmC* phase transition. The FLC investigated was *S*-(-)-2-methylbutyl 4-*n*-nonanoyloxybiphenyl-4′-carboxylate [61–66]. Its phase transition temperature sequence and structural formula are shown in figure 1. The SmC* phase appears in a broad range of temperature and can be easily supercooled to approximately 265 K (crystallization). For this material the spontaneous polarization $\mathbf{P}_s$ is about $2\,\mathrm{nC\,cm^{-2}}$. With decreasing temperature $\mathbf{P}_s$ falls rapidly to zero, inverts sign around 292 K then increases again. The helical pitch of the FLC material has been measured by a laser

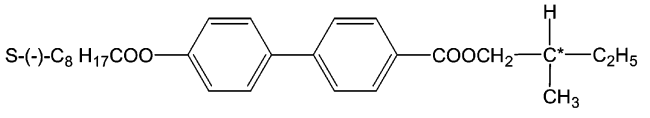

Cr—312.15 K—SmC*—315.65 K—SmA—332.65 K—I

Figure 1. Chemical structure and mesomorphism of the investigated material.

diffraction technique [62, 63] in a thick sample, about 100 μm. The helical pitch decreases with decreasing temperature from about 3.8 μm near the phase transition (315.65 K) to about 1.1 μm at 281 K. The measurements presented here were performed in the SmC* phase, in the temperature range from 315.65 K to 308 K where the helical pitch changes from about 3.8 μm to about 3.0 μm and is relatively large compared with the estimated value of the mean aerosil void size l_0. Also the optical tilt angle shows rather unusual temperature dependence [61–63].

The hydrophilic aerosil 300 (Degussa Corp.), used in the experiment, is a white, fluffy powder consisting of spherically shaped primary particles with a diameter of about 7 nm and specific surface area $a=300\,\mathrm{m^2\,g^{-1}}$. The surfaces of hydrophilic aerosil particles are covered with hydroxyl groups (–OH), which by H-bonding can form a mechanically fragile gel network at sufficiently high concentrations. The hydrophilic coating induces homeotropic orientation of the polar LC molecules at the surface [67].

The FLC–aerosil mixtures were prepared using the solvent method described in previous papers [16, 28]. The proper amount of previously heated (at 473 K) aerosil in an evacuated oven was added to a diluted solution of the FLC in spectrally pure acetone. The solution was sonicated for about one hour to obtain a homogenous dispersion of the silica in the solvent. After gradual evaporation of the solvent at about 323 K, the samples were evacuated overnight at a temperature in the SmA phase (about 323 K) to remove the remaining solvent. Five concentrations of hydrophilic aerosil were prepared, $\rho_s=0.025$, 0.05, 0.08, 0.15 and $0.2\,\mathrm{g\,cm^{-3}}$. Here $\rho_s=(m_s/m_{LC})\rho_{LC}$, where m_s and m_{LC} are the masses of aerosil and liquid crystal; $\rho_{LC}\sim 1\,\mathrm{g\,cm^{-3}}$ is the density of liquid crystal.

To examine the phase transition temperatures and transition enthalpies of the phase transitions, differential scanning calorimetry (DSC) measurements were performed. A Mettler-Toledo DSC 822e calorimeter was employed in the temperature range 233–336 K at a scan rate of $2\,\mathrm{K\,min^{-1}}$. Several milligrams of the bulk and the composite material enclosed in aluminium capsules were used for the DSC measurements. STARe software was applied to evaluate the DSC data.

The dielectric measurements were performed in the frequency range 10^{-2}–10^7 Hz, using a Novocontrol broadband dielectric spectrometer with a high resolution dielectric/impedance analyser Alpha, and an active sample cell. The samples were sandwiched directly between gold-plated electrodes separated by 50 μm glass fibre spacers. However, before final measurements the dielectric spectra were controlled in the SmC* phase

to achieve the maximum dielectric strength of the Goldstone mode. Especially in bulk measurements, the sample was slowly heated and cooled several times across the isotropic–SmA phase transition. After this procedure rather strong soft and Goldstone modes were observed which indicated that a predominant number of smectic layers were oriented in parallel to the electric field. Within this study, the bulk spectra provide only a standard for the identification and appropriate assignment of the individual processes, for which the selected geometry is satisfactory.

The orientation of the aerosil samples is difficult because the mixture is extremely viscous especially for higher concentrations of silica. Even special treatment of the electrode surfaces cannot improve orientation of the samples. Moreover, in the applied configuration of electrodes the application of the shear method to develop the LC orientation is very limited and not easy. Generally, the orientation of the smectic layers is random and the LC is distributed in domains. If a magnetic filed were used to orient the aerosil samples the magnetic induction **B** should be very high. For instance, if $\mathbf{B}=8\,\mathrm{T}$, the magnetic coherence length $\xi=\left(\frac{\mu_0 K_{33}}{\Delta\chi}\right)^{\frac{1}{2}}\frac{1}{B}$ is about 1 μm and considerably exceeds the mean aerosil void size l_0, which for silica density $0.025\,\mathrm{g\,cm^{-3}}$ is about 0.27 μm. K_{33} is the elastic constant ($\sim 2\times10^{-11}\,\mathrm{N}$), μ_0 the magnetic constant ($4\pi\times10^{-7}\,\mathrm{N\times A^{-2}}$), and $\Delta\chi$ the diamagnetic susceptibility ($\sim 2.8\times10^{-6}$). In this situation for higher silica concentrations, the influence of a magnetic field can be neglected. The measurements were performed in the temperature range 336–308 K on cooling the sample with temperature steps of about 50 mK to obtain good resolution near the SmA–SmC* phase transition.

3. Theory

In the ferroelectric chiral smectic C (SmC*) phase the molecules are tilted with respect to the layer normal. This structural change in comparison with the paraelectric SmA phase can be described by a two-dimensional order parameter with components: $\xi_1=\theta\cos\phi$ and $\xi_2=\theta\sin\phi$, were θ is the tilt angle of the molecules with respect to the smectic layer normal and the azimuthal angle ϕ defines the molecular projection in the layer plane. In the SmC* phase a helical superstructure appears with a director distribution in the z direction expressed by the equation $\phi=qz$, where $q=2\pi/p$ is the wave vector of the helix and p is the helical pitch. The external electric field $\mathbf{E}(t)=\mathbf{E}_0\exp(\mathrm{i}\omega t)$ causes a small deformation of the helix and contributes to the macroscopic polarization $\mathbf{P}_\mathrm{s}$ with dynamic azimuthal distribution described by [68–70]:

$$-\gamma_\mathrm{G}\sin^2\theta\frac{\partial\phi}{\partial t}+K_3\sin^2\theta\frac{\partial^2\phi}{\partial z^2}-\mathbf{P}_\mathrm{s}\mathbf{E}(t)\sin\phi=0 \quad (1)$$

where γ_G is the rotational viscosity of the Goldstone mode in the SmC* phase, and K_3 is the twist elastic constant. The solution of equation (1) gives the following relationships for dielectric relaxation strength $\Delta\varepsilon_\mathrm{G}$ and relaxation time τ_G of the Goldstone mode:

$$\Delta\varepsilon_\mathrm{G}=\frac{\mathbf{P}_\mathrm{s}^2}{2\varepsilon_0 K_3\theta^2 q^2} \quad (2)$$

$$\tau_\mathrm{G}=\frac{1}{2\pi f_\mathrm{G}}=\frac{\gamma_\mathrm{G}}{K_3 q^2}. \quad (3)$$

Equation (2) is derived for the idealized situation where smectic layers are parallel to the measuring electric field (helical axis perpendicular to the electric field). In the real experiment, even in bulk samples it is very difficult to prepare completely oriented samples with no defects and imperfections in orientation. In the first approximation, the difference between the theoretically predicted value of the dielectric strength of the Goldstone mode and that achieved experimentally can measure the quality of the orientation of the sample.

The double-degenerate soft mode, which occurs in the SmA phase, splits at the phase transition temperature T_AC into the Goldstone and soft amplitude modes. The dielectric strength $\Delta\varepsilon_{\mathrm{s,A}}$ and relaxation time $\tau_{\mathrm{s,A}}$ in the SmA phase ($T\geqslant T_\mathrm{AC}$) are given by the following expressions [68]:

$$\tau_{\mathrm{s,\,A}}=\frac{1}{2\pi f_{\mathrm{s,\,A}}}=\frac{\gamma_{\mathrm{s,\,A}}}{\left[a_0(T-T_\mathrm{AC})+(K_3-\varepsilon\mu^2)q_0^2\right]} \quad (4)$$

$$\varepsilon_0\Delta\varepsilon_{\mathrm{s,\,A}}=\frac{\varepsilon^2 C^2}{a_0(T-T_\mathrm{AC})+(K_3-\varepsilon\mu^2)q_0^2} \quad (5)$$

where a_0 is the phenomenological constant of the Landau free energy density expansion, $\gamma_{\mathrm{s,A}}$ is the rotational viscosity of the soft mode in the SmA phase, μ and C are coefficients of the flexoelectric and piezoelectric bilinear coupling, ε is the dielectric constant of the system in the high frequency limit [69] and ε_0 is the permittivity of free space.

For the evaluation and quantitative analysis of the dielectric spectra, the superposition of Harviliak–Negami relaxation functions and conductivity contribution was applied [71]:

$$\varepsilon^*(\omega)=\varepsilon_\infty+\sum_j\frac{\Delta\varepsilon_j}{\left[1+\left(\mathrm{i}\omega\tau_j\right)^{1-\alpha_j}\right]^{\beta_j}}-\mathrm{i}\frac{\sigma}{\varepsilon_0\omega^k} \quad (6)$$

where parameters characterizing the j-th relaxation process are the relaxation times τ_j, and the relaxation strength $\Delta\varepsilon_j$. The exponents α_j and β_j describe broadening and asymmetry of the relaxation time distribution, respectively. ε_∞ is the high frequency limit of the permittivity. The conductivity contribution described by the second term in equation (6) dominates in the low frequency range where σ is the Ohmic conductivity and k a fitting parameter.

4. Results

4.1. *Dielectric measurements*

In the applied frequency window it was possible to characterize and measure the collective relaxation processes present in the FLC. Moreover, in this study we concentrate on the evolution of the dielectric phenomena near the SmA–SmC* phase transition where the most interesting phenomena appear related to the influence of the concentration of aerosil particles on the dynamic of the collective modes. However, measurements were also performed in the broad temperature range where a rapid drop of $\Delta\varepsilon$ and disappearance of the Goldstone mode in a point of inverse of sign of spontaneous polarization was indeed detected, confirming results obtained in other experiments [62].

In the isotropic phase (I) of the bulk FLC the conductivity dominates, with a remaining wing of the molecular process on the high frequency side of the spectrum. With decreasing temperature the I–SmA phase transition occurs (at $T_{IA}=332.65\,K$) and the relaxation process related to the double-degenerate soft mode (SM) becomes visible. Near the SmA–SmC* phase transition temperature characteristic softening of the dielectric process is observed. In the SmA phase the dielectric intensity of the soft mode increases considerably with decreasing temperature. However, the characteristic frequency decreases with decreasing temperature. In the SmC* phase the double degeneracy is lifted and the soft mode splits into the Goldstone mode (GM) and the soft amplitude mode. The dielectric intensity of the SM decreases again and its frequency increases. In a very narrow range of temperature the dielectric relaxation strength of the GM increases with decreasing temperature and approaches a maximum related to the maximum of the helical superstructure in the SmC* phase. The Goldstone mode dominates in the SmC* phase with very high dielectric intensity.

In the dispersions of aerosil particles in FLC, the collective dynamics of the relaxation processes changes significantly with increasing concentration. Figure 2 presents the frequency dependence of the real and imaginary part of the dielectric function in the SmC* phase at several densities of aerosil. In the low frequency range the conductivity contributes to the spectra and a slight decrease in conductivity is observed with increasing concentration of aerosil. The observed effect is interesting because for normal 'impurities' the conductivity increases with their concentration and the phase transition temperature can be shifted several degrees. However, the introduction of inert aerosil particles to the measurement capacitor decreases the effective volume of the liquid crystal, with charge carriers therein which participate in the total conductivity of the system. In this situation with increasing concentration of aerosil the conductivity of the mixture slightly decreases. In the bulk FLC the Goldstone mode

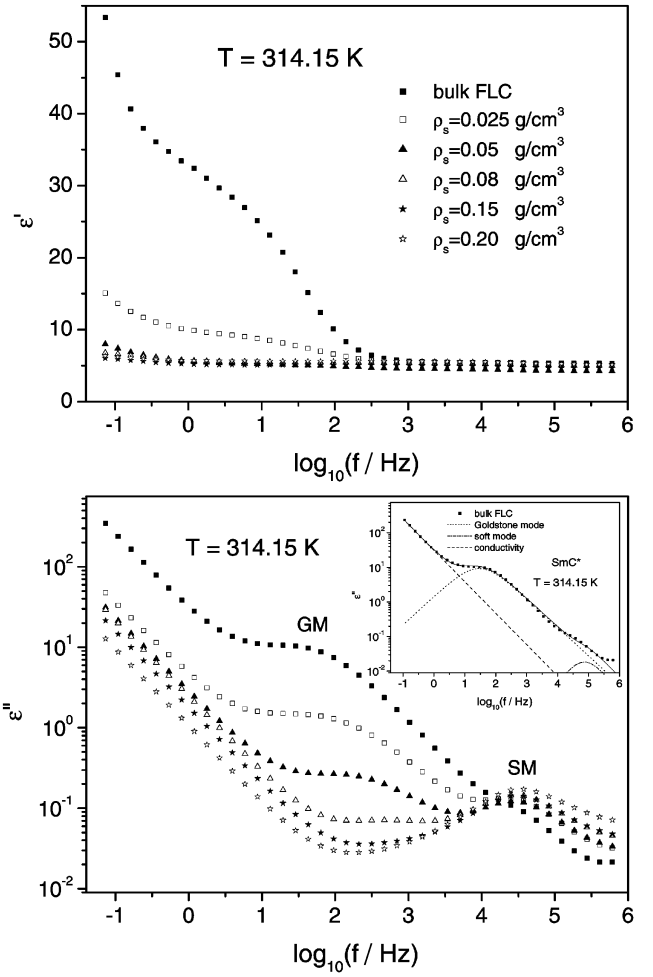

Figure 2. Comparison of the frequency dependence of (*a*) the real and (*b*) the imaginary part of the dielectric function in the SmC* phase of the bulk and dispersed FLC with different concentrations of aerosil particles. The inset in (*b*) illustrates the fitting separation result of the Goldstone mode (GM) and the soft mode (SM) for the bulk.

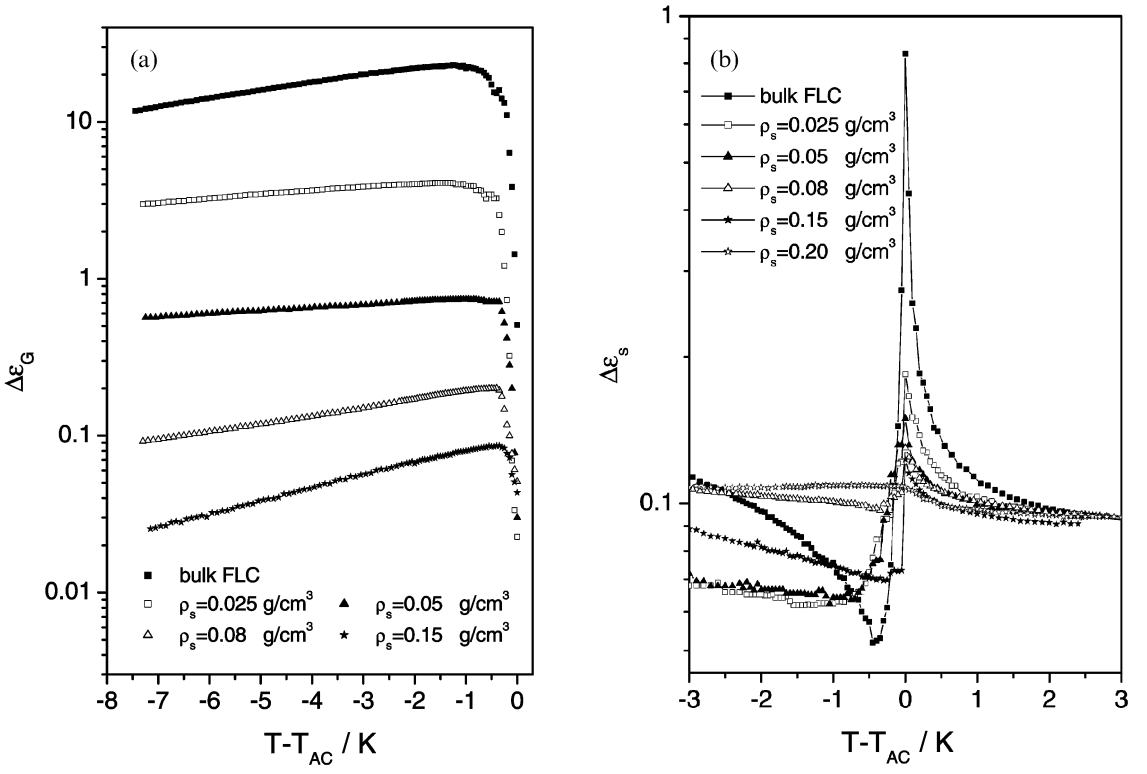

Figure 3. The temperature dependence of dielectric strength of (*a*) the Goldstone mode and (*b*) the soft mode at various concentrations of aerosil particles.

dominates and appears together with the soft amplitude mode. With increasing aerosil density ($\rho_s \leqslant 0.15\,\mathrm{g\,cm^{-3}}$) the intensity of the Goldstone mode monotonically decreases and for $\rho_s = 0.20\,\mathrm{g\,cm^{-3}}$ disappears within experimental accuracy, figure 2 (*b*). The inset in figure 2 (*b*) illustrates the fitting separation result of the Goldstone mode and the soft mode for the bulk.

Figure 3 presents the temperature dependence of the dielectric relaxation strength of the Goldstone and soft amplitude modes as obtained from fits to equation (6). The dielectric intensities of both modes continuously decrease with increasing concentration of aerosil. For the density $\rho_s = 0.20\,\mathrm{g\,cm^{-3}}$ the Goldstone mode disappears, but the soft amplitude mode is still observed although considerably broadened and with a very low intensity. The phase transition temperature $T^0_{AC} = 315.65\,\mathrm{K}$ is slightly shifted to lower temperatures with increasing aerosil concentration. The shift of the T^0_{AC} is relatively small—$\Delta T_{AC} = T^0_{AC} - T_{AC}(\rho_s) < 0.5\,\mathrm{K}$—and was determined from inspection of dielectric spectra, DSC measurements and observation of SmA–SmC* phase transition under a polarizing microscope.

The temperature dependence of relaxation frequencies for the Goldstone and soft mode are shown in figure 4. In the bulk FLC, figure 4 (*a*), the characteristic critical softening in the SmA–SmC* phase transition is visible with frequency degeneracy for the Goldstone and soft modes. The relaxation frequency for the Goldstone mode is nearly temperature independent in the employed temperature range. With increasing concentration of aerosil, figure 4 (*b*, *c*), the degeneracy in the phase transition is lifted and a gap appears, which enhances with silica density in the range from 20 kHz to about 40 kHz. The temperature dependence of the characteristic frequency of the Goldstone mode with increasing density of aerosil changes from 0.1 kHz for the bulk FLC to about 1 kHz for silica density $\rho_s = 0.15\,\mathrm{g\,cm^{-3}}$. Generally, the temperature dependence of the relaxation frequency of the Goldstone and soft modes are different in comparison with the bulk, and depends significantly on the aerosil density.

For the determination of concentration dependence of the rotational viscosity of the Goldstone mode in the SmC* phase, the temperature dependence of the product of the dielectric relaxation strength $\Delta\varepsilon_G$ and characteristic frequency f_G is shown in figure 5. This quantity is inversely proportional to the rotational viscosity. The $\Delta\varepsilon_G f_G$ decreases with decreasing temperature and with increasing concentration of aerosil. This effect is more pronounced for higher densities of silica.

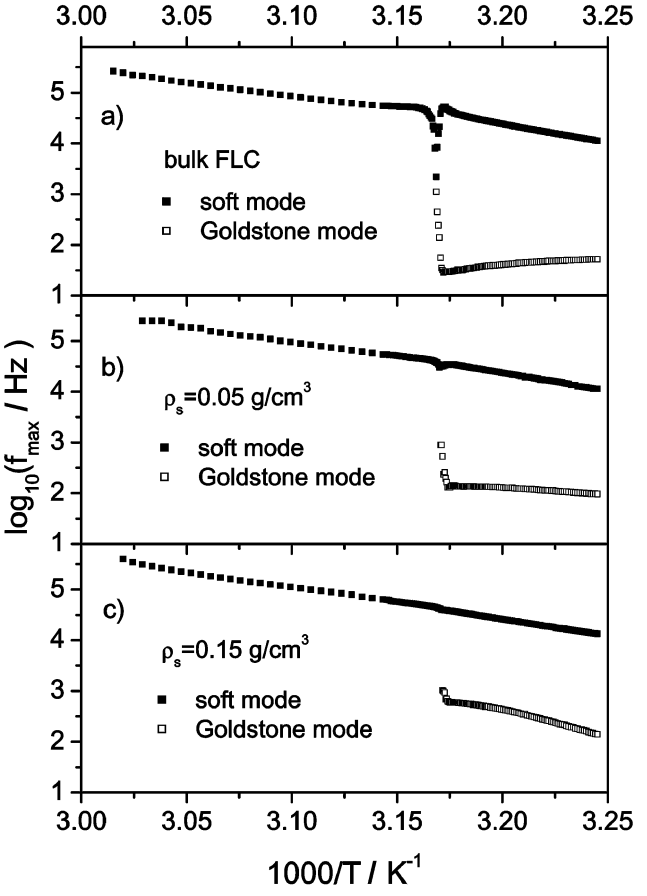

Figure 4. Temperature dependence of the characteristic relaxation frequencies deduced from fits to equation (6) for various densities of aerosil particles.

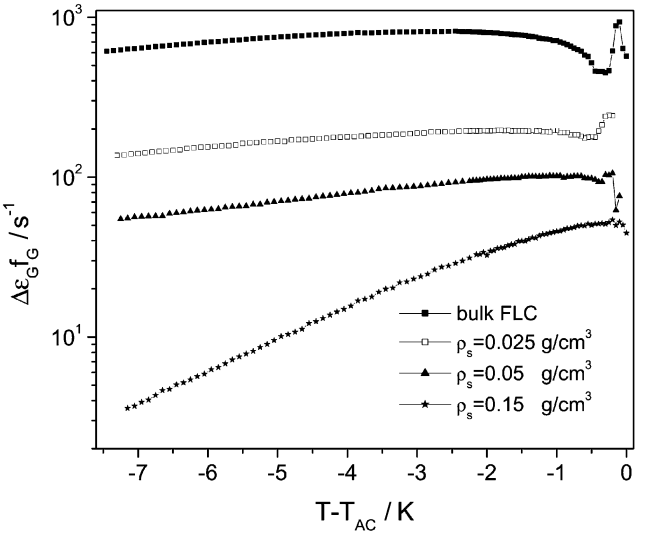

Figure 5. Temperature dependence of the product of $\Delta\varepsilon_G$ and f_G at various concentrations of aerosil particles.

4.2. *DSC measurements*

The DSC measurements were carried out for the bulk FLC and for mixtures with silica aerosil at several concentrations. During heating, the phase sequence was Cr–SmA–I and the SmC* phase was not detected. However, during a second heating run a weak peak related to the SmA–SmC* phase transition was visible. On cooling, the sequence of phases was I–SmA–SmC*–Cr, and the smectic C* phase appeared in very broad range of temperature down to 265 K where the FLC started to crystallize. The transition enthalpies and temperatures given in table 1 reveal no significant changes with increasing concentration of aerosil up to $\rho_s = 0.20\,\mathrm{g\,cm^{-3}}$. However, the SmA–SmC* phase transition is slightly shifted to lower temperatures and the transition peak continuously broadened with increasing concentration of aerosil (figure 6). The very weak peak in the SmA–SmC* phase transition is characteristic for a second order phase transition. For higher silica concentrations the SmA–SmC* peaks become very

Table 1. Phase transition temperatures and enthalpies extracted from the DSC curves.

		T_{onset} (T_{peak})/K						ΔH/ J g^{-1}					
			ρ_s/g cm^{-3}						ρ_s/g cm^{-3}				
Run	Phase	Bulk	0.025	0.05	0.08	0.15	0.20	Bulk	0.025	0.05	0.08	0.15	0.20
Heating	Cr–SmA	312.13 (313.05)	311.88 (314.45)	311.66 (313.68)	310.67 (313.61)	309.71 (312.58)	308.93 (312.62)	99.6	103.5	89.9	84.3	69.6	72.5
	SmA–I	332.28 (332.60)	332.04 (332.67)	332.04 (332.68)	331.79 (332.96)	331.70 (332.80)	331.41 (332.74)	16.0	16.0	15.1	14.0	12.1	12.2
Cooling	I–SmA	332.22 (332.12)	332.12 (331.86)	332.09 (331.88)	332.06 (330.87)	331.95 (330.95)	331.74 (330.58)	16.5	15.5	15.4	14.6	12.0	12.7
	SmA–SmC*	315.58 (315.30)	315.33 (314.81)	315.31 (314.65)	315.50 (313.79)	315.61 (313.82)	315.34 (313.36)	0.9	1.0	1.1	1.1	0.6	0.3
	SmC*–Cr	266.76 (265.62)	270.07 (268.82)	269.97 (268.83)	269.78 (268.66)	269.36 (268.20)	269.03 (268.11)	26.6	26.1	25.6	24.9	20.6	21.4

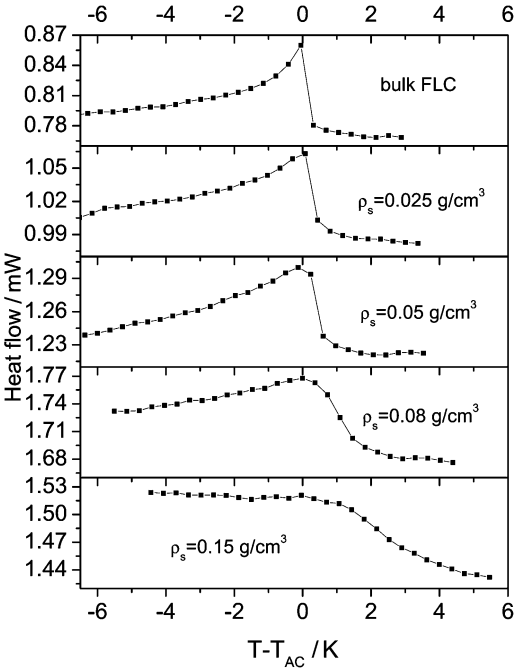

Figure 6. Comparison of the SmA–SmC* phase transition DSC peaks for several concentrations of aerosil particles.

broad which causes difficulties in correctly determining the phase transition temperature and enthalpy. The values presented in table 1 thus have a relatively large uncertainty. More pronounced changes are observed for melting and crystallization peaks.

5. Discussion

The structures created by hydrogen-bonded aerosil particles in dispersed LCs depend on the silica density, and vary from LCs in Synpor membranes [4] to LCs in aerogel [7]. In FLCs the helical pitch provides a natural scale length to estimate the effective of boundary interactions on the dynamics of the collective modes. Moreover, the helical superstructure is very sensitive to external fields and the imposed geometrical restrictions. With decreasing sample thickness the helix can be distorted and for a certain critical thickness (comparable to the pitch) the helix is completely unwound as a result of surface-induced effects. The geometrical parameters characterizing the gel structure of the FLC–aerosil systems are summarized in table 2, where $l_0=2/(a\rho_s)$ is the mean aerosil void size and $p=l_b a\rho_s$ is the fraction of 'frozen' FLC molecules anchored by the silica surface. The parameters l_0 and p were calculated taking into account a specific surface $a=300\,m^2\,g^{-1}$ and a boundary layer thickness $l_b=2\,nm$ (the order of molecular length). For the densities ρ_s just above the gelation threshold ($\rho_s=0.025\,g\,cm^{-3}$) the estimated void sizes are comparable to that of nitrocellulose porous membranes used in previous experiment [4, 5, 36, 56], where strong modifications of collective processes were observed.

Table 2. Parameters characterizing the aerosil structure and shift of the phase transition temperature. For the bulk FLC the phase transition temperature $T^0_{AC}=315.65\,K$.

$\rho_s/g\,cm^{-3}$	$T_{AC}(\rho_s)/K$	$l_0=2/(a\rho_s)/nm$	$p=l_p a\rho_s$
0.025	315.39 ± 0.02	267	0.02
0.05	315.34 ± 0.02	133	0.03
0.08	315.29 ± 0.02	83	0.05
0.15	315.21 ± 0.02	44	0.09
0.20	315.30 ± 0.05	33	0.12

The hydrogen-bonded silica inclusions in the FLC form a very complicated and disordered structure acting as a random field. The system of voids and strands can significantly change orientational order and molecular dynamics in the boundary layers and enforce boundary conditions on the director field. These interactions depend on the properties of the surface and liquid crystal. The length scales and geometrical shape of voids also play a significant role [72, 73]. The presence of disordered surfaces in a LC produces elastic strain that increases with aerosil density. Moreover, the hydrophilic silica spheres anchor LC molecules and immobilize them on the surface.

Under the influence of the aerosil the LC is divided into rather large but finite domains distributed in space. This was demonstrated in static light scattering studies of aerosil–nematic liquid crystal dispersions [74]. The smectic layers form within these domains and, depending on the sizes of the domains, a helical superstructure more or less distorted by the surface interactions can be created. The frequency dependence of the Goldstone mode is almost unaffected by low concentrations of aerosil, and comes from rather large domains comparable to the helical pitch. However, with increasing density, up to $\rho_s \leqslant 0.15\,g\,cm^{-3}$, a shift to higher frequencies is observed, indicating a decrease of the domain size, which becomes comparable to or lower than the helical pitch. In this situation the helix is strongly deformed and partially unwounded, which results in increasing frequency and decrease of relaxation strength. The dielectric relaxation strength of Goldstone and soft modes decreases with density of the silica particles because the orientation of the smectic domains becomes more homogenous in space; fewer domains are therefore oriented in the preferential direction to the measuring electric field. Additionally, the domain dimensions decrease and more LC molecules are immobilized by surface interactions. It should be noted that Goldstone and soft modes were detected

for the FLC confined in aerogel with densities of 0.08 and 0.17 g cm^{-3} with pore chords about 70 and 43 nm, respectively [7]. For a critical density the Goldstone mode disappears because the disordered defect structure prevents the formation of a helical structure. The exact determination of critical density requires the preparation of samples with very small changes in concentration of silica in the mixture. Moreover, silica gel during confinement between measuring electrodes is subjected to strong shear forces and its structure can be considerably changed and cracked. This effect is especially important for higher concentration of aerosil and can influence the value of the critical density of silica in which the Goldstone mode disappears.

With increasing silica concentration an increase in the Goldstone mode rotational viscosity of the SmC* phase (figure 5) can be expected. The evaluation of the rotational viscosity is possible from the measured values of the spontaneous polarization, tilt, dielectric strength and the characteristic relaxation frequency of the Goldstone mode. The relation between these quantities derived from equations (2) and (3) is given by:

$$\gamma_G = \mathbf{P}_s^2 / \left(4\pi\varepsilon_0\theta^2\Delta\varepsilon_G f_G\right). \quad (7)$$

In the measured temperature range the tilt angle θ increase from 0 to about 0.3 rad and $\mathbf{P}_s$ approaches a maximum at 1.95 nC cm^{-2} [61]. The rotational viscosity γ_G at a temperature of 311 K, calculated from equation (7), changes from 0.06 N s m^{-2} in the bulk FLC to about 3 N s m^{-2} for ρ_s=0.15 g cm^{-3}. This considerable change in rotational viscosity and the previously described effects can substantially influence the dynamics of the Goldstone mode.

The change in the characteristic frequency of the soft mode at the phase transition, and the increasing gap with increasing density of silica particles, can be related to the deformation of the smectic layers, enforced by competition between elastic forces and strong surface interactions. The hydrophilic silica spheres dispersed in liquid crystal create defects in the arrangement of smectic layers and deform them especially near the surface (the diameter of aerosil particle is about 7 nm and thickness of smectic layer is about 2–3 nm). This effect is enhanced by the very huge surface of aerosils and can be detected in dielectric spectroscopy. Recently, it was shown in a high resolution X-ray scattering experiment that even a weakly connected gel could destroy smectic long range order [37]. It is known that the introduction of 'impurities' into a liquid crystal can considerably shift phase transition temperatures. However, in the case of aerosil, the experimentally observed shift of the SmA–SmC* phase transition temperature is relatively small and is about $\Delta T_{AC}\sim 0.5$ K. The distortion of smectic layers can also influence the SmA–SmC* phase transition temperature. This idea has already been discussed and applied in [3]. The frequency gap Δf_s, related to the shift of the phase transition temperature ΔT_{AC} in different domains, can be approximately determined from equation (4) as: $\Delta f_s \approx a_0 \Delta T_{AC}/2\pi\gamma$. For typical values of material constants: $a_0\sim 5\times 10^4$ N m^{-2} K [69], $\gamma\sim 0.1$ N s m^{-2}, one finds $\Delta f_s\sim 80$ kHz which is roughly the order of magnitude of the frequency shift observed in our experiment.

The DSC measurements reveal the influence of aerosil particles on the thermodynamic properties of a FLC. The phase transition temperatures and enthalpies differ only slightly from those of pure FLC, but substantial smearing-out effects are observed.

6. Conclusions

Even very low concentrations of aerosil particles considerably influence and change the dynamics of collective processes near the SmA–SmC* phase transition. The dielectric relaxation strengths of the Goldstone and soft modes decrease with increasing silica density, and for higher concentrations the Goldstone mode is totally suppressed. The soft mode dielectric strength stays very low and is considerably spread out. The temperature dependence of the relaxation frequency reveals several interesting features: (i) at the SmA–SmC* phase transition a frequency degeneracy is observed in the bulk FLC, which is lifted in the presence of aerosil; (ii) the frequency gap increases with increasing silica concentration, which can be related to the deformation of smectic layers by aerosil spheres; (iii) the relaxation frequency for the Goldstone mode is shifted slightly to higher frequencies, which suggests competition between the characteristic scale lengths related to the helical superstructure and void dimensions created by the aerosil gel. The phase transition temperatures and enthalpies for mixtures differ only slightly from the bulk FLC values, but considerable broadening is observed.

The influence of aerosil structure on the smectic phase can be considered as an effect of a random field introduced to the LC. Also the influence of disorder due to silica particles on smectic layer arrangements cannot be excluded.

We attribute the observed dynamic behaviour to several effects, which can have an influence on the LC phases. The strong homeotropic anchoring of LC molecules on the hydrophilic surface of silica spheres significantly influences the orientational order. This surface effect increases with increasing concentration of aerosil, and the surface order can be transferred to the bulk material. It is accompanied by decreasing size of

the domains as well as with a more isotropic distribution in space. The surfaces and structures produced by hydrogen-bonded silica agglomerates are not smooth and introduce significant disorder to the liquid crystal. This creates complicated structures of irregular interconnected voids and strands with very rough surfaces. These boundaries create defects in the director and layer structures. Another important role played by these systems concerns the finite size effects related to the competition between the helical superstructure, characterized by helical pitch, and mean aerosil void size l_0. With decreasing l_0 the helix is subjected to deformation and is gradually unwound with increasing concentration of silica. In this situation, depending on the value of the helical pitch, the critical density of the aerosil for which the Goldstone mode disappears should be different for different FLC materials.

Acknowledgements

This work has been supported by the National Fund for Scientific Research Flanders, Belgium (FWO, project G.0246.02). S.A.R. acknowledges the receipt of a senior postdoctoral fellowship from the Research Council of K.U.Leuven. The authors are indebted to K. Lodewyckx for help in DSC measurements.

References

[1] G.P. Crawford, S. Žumer (editors). *Liquid Crystals in Complex Geometries*. Taylor & Francis, London, Bristol (1996).
[2] K.L. Sandhya, S. Krishna Prasad, D.S. Shankar Rao, Ch. Bahr. *Phys. Rev. E*, **66**, 031710 (2002).
[3] Z. Kutnjak, S. Kralj, S. Žumer. *Phys. Rev. E*, **66**, 041702 (2002).
[4] S.A. Różański, R. Stannarius, F. Kremer, S. Diele. *Liq. Cryst.*, **28**, 1071 (2001).
[5] S.A. Różański, R. Stannarius, F. Kremer. *IEEE Trans. Dielectr. Electr. Insul.*, **8**, 488 (2001).
[6] L. Naji, F. Kremer, R. Stannarius. *Liq. Cryst.*, **25**, 363 (1998).
[7] H. Xu, J.K. Vij, A. Rappaport, N.A. Clark. *Phys. Rev. Lett.*, **79**, 249 (1997).
[8] V. Novotna, M. Glogarova, A.M. Bubnov, H. Sverenyak. *Liq. Cryst.*, **23**, 511 (1997).
[9] F.M. Aliev, J. Kelly. *Ferroelectrics*, **151**, 263 (1994).
[10] Yu.P. Panarin, Yu.P. Kalmykov, S.T. Mac Lughadha, H. Xu, J.K. Vij. *Phys. Rev. E*, **50**, 4763 (1994).
[11] T. Povše, I. Muševic, B. Žekš, R. Blinc. *Liq. Cryst.*, **14**, 1587 (1993).
[12] K. Kondo, H. Takezoe, A. Fukuda, E. Kuze. *Jpn. J. appl. Phys.*, **21**, 224 (1982).
[13] K. Kondo, H. Takezoe, A. Fukuda, E. Kuze, K. Flatischer, K. Skarp. *Jpn. J. appl. Phys.*, **22**, L294 (1983).
[14] P. Jamee, G. Pitsi, J. Thoen. *Phys. Rev. E*, **66**, 021707 (2002).
[15] G.S. Iannacchione, C.W. Garland, J.T. Mang, T.P. Rieker. *Phys. Rev. E*, **58**, 5966 (1998).
[16] H. Haga, C.W. Garland. *Liq. Cryst.*, **23**, 645 (1997).
[17] B. Zhou, G.S. Iannacchione, C.W. Garland, T. Bellini. *Phys. Rev. E*, **55**, 2962 (1997).
[18] S. Qian, G.S. Iannacchione, D. Finotello. *Phys. Rev. E*, **57**, 4305 (1998).
[19] Z. Kutnjak, C.W. Garland. *Phys. Rev. E*, **55**, 488 (1997).
[20] G.S. Iannacchione, D. Finotello. *Phys. Rev. Lett.*, **69**, 2094 (1992).
[21] B. Zalar, R. Blinc, S. Žumer, T. Jin, D. Finotello. *Phys. Rev. E*, **65**, 041703 (2002).
[22] T. Jin, D. Finotello. *Phys. Rev. Lett.*, **86**, 818 (2001).
[23] G.S. Iannacchione, G.P. Crawford, S. Qian, J.W. Doane, D. Finotello, S. Žumer. *Phys. Rev. E*, **53**, 2402 (1996).
[24] R.J. Ondris-Crawford, M. Ambrožič, J.W. Doane, S. Žumer. *Phys. Rev. E*, **50**, 4773 (1994).
[25] G.P. Crawford, R. Stannarius, J.W. Doane. *Phys. Rev. A*, **44**, 2558 (1991).
[26] M.A. Zaki Ewiss, G. Nabil, B. Stoll, S. Herminghaus. *Liq. Cryst.*, **30**, 1241 (2003).
[27] A. Hourri, P. Jamee, T.K. Bose, J. Thoen. *Liq. Cryst.*, **29**, 459 (2002).
[28] A. Hourri, T.K. Bose, J. Thoen. *Phys. Rev. E*, **63**, 051702 (2001).
[29] S. Frunza, L. Frunza, H. Goering, H. Sturm, A. Schönhals. *Europhys. Lett.*, **56**, 801 (2001).
[30] F. Kremer, A. Huwe, A. Schönhals, S.A. Różański. *Broadband Dielectric Spectroscopy*. F. Kremer, A. Schönhals (Eds), pp. 171–224, Berlin, Heidelberg, New York: Springer-Verlag (2003).
[31] S.A. Różański, R. Stannarius, H. Groothues, F. Kremer. *Liq. Cryst.*, **20**, 59 (1996).
[32] S.A. Różański, R. Stannarius, F. Kremer. *Z. Phys. Chem.*, **211**, 147 (1999).
[33] G.P. Sinha, F.M. Aliev. *Phys. Rev. E*, **58**, 2001 (1998).
[34] Ch. Cramer, Th. Cramer, F. Kremer, R. Stannarius. *J. chem. Phys.*, **106**, 3730 (1997).
[35] S.L. Abd-El-Messieh, J. Werner, H. Schmalfuss, W. Weissflog, H. Kresse. *Liq. Cryst.*, **26**, 535 (1999).
[36] S.A. Różański, L. Naji, F. Kremer, R. Stannarius. *Mol. Cryst. liq. Cryst.*, **329**, 483 (1999).
[37] S. Park, R.L. Leheny, R.J. Birgeneau, J.-L. Gallani, C.W. Garland, G.S. Iannacchione. *Phys. Rev. E*, **65**, 050703 (2002).
[38] C.C. Retsch, I. McNulty, G.S. Iannacchione. *Phys. Rev. E*, **65**, 032701 (2002).
[39] G.S. Iannacchione, J.T. Mang, S. Kumar, D. Finotello. *Phys. Rev. Lett.*, **73**, 2708 (1994).
[40] K. Kočevar, I. Muševič. *Phys. Rev. E*, **64**, 051711 (2001).
[41] A. Hauser, H. Kresse, A. Glushchenko, O. Yaroshchuk. *Liq. Cryst.*, **26**, 1603 (1999).
[42] W.I. Goldburg, F. Aliev, X.-l. Wu. *Physica A*, **213**, 61 (1995).
[43] T. Bellini, N.A. Clark, Light scattering as a probe of liquid crystal ordering in silica aerogels, in [10] and refs. therein.
[44] G.P. Crawford, L.M. Steele, R. Ondris-Crawford, G.S. Iannacchione, C.J. Yeager, J.W. Doane, D. Finotello. *J. chem. Phys.*, **96**, 7788 (1992).
[45] C. Charcosset, J.-C. Bernengo. *J. Membr. Sci.*, **168**, 53 (2000).
[46] L. Cipelletti, M. Carpineti, M. Giglio. *Langmuir*, **12**, 6446 (1996).
[47] P. Levitz, G. Ehret, S.K. Sinha, J.M. Drake. *J. chem. Phys.*, **95**, 6151 (1991).

[48] M. Vilfan, T. Apih, A. Gregorovič, B. Zalar, G. Lahajnar, S. Žumer, G. Hinze, R. Böhmer, G. Althoff. *Magn. Reson. Img.*, **19**, 433 (2001).
[49] T.H. Elmer. *Engineered Materials Handbook*, Vol. 4, Ceramic and Glasses, Ohio: ASM International, pp. 427–432 (1992).
[50] S.M. Kelly. *Liq. Cryst.*, **24**, 71 (1998).
[51] T. Bellini, L. Radzihovsky, J. Toner, N.A. Clark. *Science*, **294**, 1074 (2001).
[52] A. Borštnik, H. Stark, S. Žumer. *Phys. Rev. E*, **60**, 4210 (1999).
[53] L. Radzihovsky, J. Toner. *Phys. Rev. Lett.*, **78**, 4414 (1997).
[54] L. Radzihovsky, J. Toner. *Phys. Rev. Lett.*, **79**, 4214 (1997).
[55] S.A. Różański, R. Stannarius, F. Kremer. *Proc. SPIE*, **4759**, 178 (2001).
[56] S.A. Różański, L. Naji, R. Stannarius, F. Kremer. *Proc. SPIE*, **3488**, 36 (1997).
[57] S.A. Różański. *Phys. Stat. Sol. (a)*, **79**, 309 (1983).
[58] S.A. Różański, W. Kuczyński. *Chem. Phys. Lett.*, **105**, 104 (1984).
[59] I. Muševič, B. Žekš, R. Blinc, T. Rasing, P. Wyder. *Phys. Rev. Lett.*, **48**, 192 (1982).
[60] B. Žekš, R. Blinc. *Ferroelectricity and Related Phenomena*, Vol. 7, pp. 365–407, Gordon and Breach, Amsterdam (1991).
[61] J.W. Goodby, E. Chin, J.M. Geary, J.S. Patel, P.L. Finn. *J. chem. Soc. Faraday Trans.*, **83**, 3429 (1987).
[62] R. Eidenschink, T. Geelhaar, G. Andersson, A. Dahlgren, K. Flatischler, F. Gouda, S.T. Lagerwall, K. Skarp. *Ferroelectrics*, **84**, 167 (1988).
[63] I. Muševič, I. Drevenšek, R. Blinc, S. Kumar, J.W. Doane. *Mol. Cryst. liq. Cryst.*, **172**, 217 (1989).
[64] K. Skarp, K. Flatischler, S.T. Lagerwall. *Ferroelectrics*, **84**, 183 (1988).
[65] W.G. Jang, C.S. Park, J.E. Maclennan, K.H. Kim, N.A. Clark. *Ferroelectrics*, **180**, 213 (1996).
[66] Ch. Bahr, C.J. Booth, D. Fleigner, J.W. Goodby. *Ferroelectrics*, **178**, 229 (1996).
[67] M. Marinelli, A.K. Ghosh, F. Mercuri. *Phys. Rev. E*, **63**, 061713 (2001).
[68] A. Levstik, Z. Kutnjak, C. Filipič, I. Levstik, Z. Bregar, B. Žekš, T. Carlsson. *Phys. Rev. A*, **42**, 2204 (1990).
[69] T. Carlsson, B. Žekš, C. Filipič, A. Levstik. *Phys. Rev. A*, **42**, 877 (1990).
[70] R. Blinc, B. Žekš. *Phys. Rev. A*, **18**, 740 (1978).
[71] A. Schönhals, F. Kremer. *Broadband Dielectric Spectroscopy*. F. Kremer, A. Schönhals (Eds), pp. 59–98, Berlin, Heidelberg, New York: Springer-Verlag (2003).
[72] G.S. Iannacchione, S. Park, C.W. Garland, R.J. Birgeneau, R.L. Leheny. *Phys. Rev. E*, **67**, 011709 (2003).
[73] R.L. Leheny, S. Park, R.J. Birgeneau, J.-L. Gallani, C.W. Garland, G.S. Iannacchione. *Phys. Rev. E*, **67**, 011708 (2003).
[74] T. Bellini, N.A. Clark, V. Degiorgio, F. Mantegazza, G. Natale. *Phys. Rev. E*, **57**, 2996 (1998).